Spectral properties of partially coherent chirped Airy pulsed beam in oceanic turbulence*

ZHU Bo-yuan (朱博源), **BIAN Shao-jie** (边绍杰), **TONG Yang** (童阳), **MOU Xin-yue** (牟新月), **and CHENG Ke** (程科)**

College of Optoelectronic Technology, Chengdu University of Information Technology, Chengdu 610225, China

(Received 19 February 2020; Revised 16 April 2020)

Spectral shifts and spectral intensities of partially coherent chirped Airy pulsed (PCCAP) beams propagating through oceanic turbulence are studied, where spectral properties of partially coherent chirped Gaussian pulsed (PCCGP) beams are also compared. The effects of optical parameters and oceanic turbulence parameters on spectral shifts at different observation positions are mainly discussed. It is shown that the spectral shift of PCCAP beam is richer than that of PCCGP beam, and there exists some critical positions for PCCAP beams where the spectral red-shift reaches its maximum. The spectral red-shift increases with increasing chirped parameter, correlation length or decreasing pulse duration. However, the increasing of spectral red-shift is accompanied by increasing dissipation rate of turbulence kinetic energy in unit mass liquid or decreasing relative intensity of temperature and salinity fluctuations, mean square temperature dissipation rate. A physical explanation of rapid spectral transition is also made.

Document code: A **Article ID:** 1673-1905(2021)02-0123-6

DOI https://doi.org/10.1007/s11801-021-0027-4

There has been recently extensive interest in studying propagation of laser beams in oceanic turbulence due to their applications in underwater optical communication, imaging and sensing[1]. The intensity evolution, spectral behavior, polarization properties, underwater ghost imaging and beam wander of various laser beams propagating in turbulent ocean were studied[2-23]. For example, Ding et al[9] studied the spectral switches of two-dimensional spatially and temporally partially coherent Gaussian Schell-model (GSM) pulsed beams propagation in oceanic turbulence and showed that the oceanic turbulence-induced spectral switches can be affected by dissipation rate of turbulence kinetic energy in unit mass liquid, decreasing relative intensity of temperature and salinity fluctuations and mean square temperature dissipation rate. Liu et al[22] investigated the averaged intensity and coherence properties of partially coherent anomalous hollow vortex beams in underwater oceanic turbulence. Sun et al[23] explored the statistical properties of partially coherent polarized Gaussian beams in oceanic turbulence with anisotropy.

On the other hand, some diffraction-free beams such as Bessel, Airy beams and their families have better abilities to reduce atmospheric turbulence effects[24,25]. In the domain of ultra-short pulse optical wavefield, the effect of oceanic turbulence on spectral properties of fully coherent chirped Gaussian pulsed beam was investigated by Liu et al[6] who showed that depending on the optical parameters, i.e., pulse duration and chirp parameter, and oceanic turbulence parameters, the blue or red-shifted spectrum can be achieved. Interesting is to ask: what will happen if a chirped Gaussian pulsed form is introduced to partially coherent diffraction-free Airy optical wavefield?

The purpose of this paper is to explore spectral behaviors of partially coherent chirped Airy pulsed (PCCAP) beams in oceanic turbulence. Meanwhile, we also make a comparison with the corresponding study for the case of partially coherent chirped Gaussian pulsed (PCCGP) beams. The results show that oceanic turbulence-induced spectral shifts can be found, and spectral shifts of PCCAP beams are richer than those of PCCGP beams, which also provide potential application in underwater optical communication, imaging and sensing by diffraction-free Airy pulsed beam.

Assume that an Airy pulsed beam propagates toward the half space $z\geq 0$ in oceanic turbulence. In the Cartesian coordinate system, the initial field of the Airy pulsed beam in the space-time domain at the input of $z=0$ is written as[26]:

$$E_0(x_1,0,t)=Ai\left(\frac{x_1}{x_0}\right)\exp\left(\frac{ax_1}{x_0}\right)f(t), \tag{1}$$

* This work has been supported by the Sichuan Science and Technology Program (No.2020YJ0431).

** E-mail: ck@cuit.edu.cn

where Ai is the Airy function, x_0 is an transverse scale, aperture coefficient a>0 enables the finite energy in experimental realization. In Eq.(1) the incident pulsed beam is assumed as a chirped Gaussian one given by[27]

$$f(t)=\exp\left[-\frac{(1+\mathrm{i}C)t^2}{2T^2}\right]\exp(-\mathrm{i}\omega_0 t), \tag{2}$$

where ω_0, T and C denote central frequency, pulse duration and chirp parameter, respectively.

In the space-frequency domain, the initial field of Airy pulsed beam with the angular frequency ω can be obtained by Fourier transform

$$E_0(x_1,0,\omega)=\frac{1}{2\pi_0}\int_{-\infty}^{\infty}E_0(x_1,0,t)\exp(-\mathrm{i}\omega t)\mathrm{d}t\cdot \tag{3}$$

Substituting Eqs.(1) and (2) into Eq.(3), we can obtain the initial field of space-frequency domain as

$$E_0(x_1,0,\omega)=f(\omega)Ai\left(\frac{x_1}{x_0}\right)\exp\left(\frac{ax_1}{x_0}\right), \tag{4}$$

and the power spectrum of the resulting beam as

$$S_{00}(\omega)=\left|f(\omega)\right|^2, \tag{5}$$

with the Fourier spectrum of

$$f(\omega)=\frac{1}{\sqrt{2\pi}}\sqrt{\frac{T}{1+\mathrm{i}C}}\exp\left[-\frac{T(\omega-\omega)}{2(1+\mathrm{i}C)}\right]. \tag{6}$$

The cross-spectral density function of the initial spatially partially coherent chirped Airy pulsed beams at the plane z=0 is expressed as

$$W_0(x_1,x_2,0,\omega)=\left\langle E_0(x_1,0,\omega)E_0^*(x_2,0,\omega)\right\rangle=$$
$$S^{00}(\omega)\exp\left[-\frac{(x_1-x_2)^2}{\sigma^2}\right]\prod_{\chi=x_1,x_2}Ai\left(\frac{\chi}{x_0}\right)\exp\left(\frac{a\chi}{x_0}\right), \tag{7}$$

where asterisk denotes the complex conjugation and σ is correlation length.

According to extended Huygens-Fresnel principle, the cross-spectral density function of PCCAP beams propagating through oceanic turbulence can be expressed as[6]

$$W(x_1',x_2',z,\omega)=\frac{k}{2\pi z}\iint\mathrm{d}x_1'\mathrm{d}x_2'W_0(x_1,x_2,0,\omega)\times$$
$$\exp\left\{\frac{\mathrm{i}k}{2z}\left[\left(x_1^2-x_2^2\right)+\left(x_1'^2-x_2'^2\right)-2\left(x_1x_1'-x_2x_2'\right)\right]\right\}\times$$
$$\left\langle\exp\left[\psi(x_1',x_1)+\psi^*(x_2',x_2)\right]\right\rangle_m, \tag{8}$$

where k=ω/c represents the wavenumber associated with frequency ω and speed of light in vacuum c, and ψ is the phase function depending on the refractive-index fluctuations of the medium. The statistical average of the turbulent medium statistics in Eq.(8) is given by

$$\left\langle\exp\left[\psi(x_1',x_1)+\psi^*(x_2',x_2)\right]\right\rangle_m\approx$$
$$\exp\left[-\frac{\left(x_1'-x_2'\right)^2+\left(x_1'-x_2'\right)\left(x_1-x_2\right)+\left(x_1-x_2\right)^2}{\rho_0^2}\right], \tag{9}$$

where ρ_0 is the spatial coherence length of a spherical wave propagating through oceanic turbulence, which takes the form[22,23]

$$\rho_0=\left[1.28\times10^{-8}k^2z\eta^{-1/3}\chi_T\varepsilon^{-1/3}\times\right.$$
$$\left.\left(6.78+47.57\varsigma^{-2}-17.67\varsigma^{-1}\right)\right]^{-1/2}. \tag{10}$$

Here η denotes the Kolmogorov micro scale (inner scale), χ_T is the mean square temperature dissipation rate with the range from 10^{-10} K^2/s to 10^{-4} K^2/s, ε indicates dissipation rate of turbulence kinetic energy in unit mass liquid, and its value is found to be in range of 10^{-10} m^2/s^3 to 10^{-1} m^2/s^3 (corresponding to deep water and ocean surface, respectively), ς is relative intensity of temperature and salinity fluctuations and its range is between –5 to 0 (corresponding to temperature-induced and salinity-induc-ed turbulence, respectively)[15-17].

By substituting Eqs.(7), (9) and (10) into Eq.(8) and letting x_1=x_2=x, the approximate analytical spectral intensity of PCCAP beams propagating through the oceanic turbulence at z plane is expressed as

$$S_a(x,z,\omega)=S_{00}(\omega)\times M_a(x,z,\omega), \tag{11}$$

where

$$M_a(x,z,\omega)=\exp\left(\tau\beta^2+\frac{\rho^2\alpha^2}{4}\right)\exp\left[\mathrm{i}\left(\frac{2}{3}E_{11}^3-E_{11}\times E_{21}\right)\right]\times$$
$$\exp\left[\mathrm{i}\left(\frac{2}{3}E_{12}^3-E_{12}\times E_{22}\right)\right]Ai\left(E_{21}-E_{11}^2\right)Ai\left(E_{22}-E_{12}^2\right), \tag{12}$$

$$\alpha=\frac{\mathrm{i}\omega x}{zc},\ \beta=\frac{2a}{x}-\frac{\mathrm{i}\omega\alpha\rho}{2zc}, \tag{13}$$

$$E_{11,12}=\frac{\mathrm{i}\tau}{x_0^2}\pm\frac{\omega\rho^2\tau}{2x_0^2zc}, \tag{14}$$

$$E_{21,22}=\frac{\alpha\rho^2}{4x_0^2}+\frac{2\beta\tau}{x_0}\pm\frac{\mathrm{i}\omega\rho^2\beta\tau}{2x_0^2zc}, \tag{15}$$

$$\frac{1}{\rho^2}=\frac{1}{\sigma^2}+\frac{1}{\rho_0^2},\ \tau=\left(\frac{z\omega}{c\rho}\right)^2. \tag{16}$$

For E_{11} and E_{22} in Eqs.(14) and (15), their signs are negative, while for E_{12} and E_{21}, the signs are positive, respectively.

For comparison, the spectral intensity of PCCGP beams using the same method is also further given by

$$S_g(x,z,\omega)=S_{00}(\omega)\times M_g(x,z,\omega), \tag{17}$$

where

$$M_g(x,z,\omega)=\frac{\omega}{2zc\sqrt{AB}}\exp(-\frac{\omega^2x^2}{4Azc^2})\times$$
$$\exp\left[\frac{1}{4B}\left(\frac{1}{A\rho^2}-1\right)^2\left(\frac{\mathrm{i}\omega x}{zc}\right)^2\right], \tag{18}$$

$$A=\frac{1}{x_0^2}+\frac{1}{\rho^2}+\frac{\mathrm{i}\omega}{2zc},\ B=\frac{1}{x_0^2}+\frac{1}{\rho^2}+\frac{\mathrm{i}\omega}{2zc}-\frac{1}{A\rho^4}. \tag{19}$$

In Eqs.(11) and (17), $M_i(x, z, \omega)$ (i=a or g) is called as spectral modifiers. One can see that the spectral intensities of PCCAP and PCCGP beams in oceanic turbulence are determined by both original spectrum $S_{00}(\omega)$ and spectral

modifier $M_i(x, z, \omega)$, respectively, where the first part $S_{00}(\omega)$ depends on pulse duration T and chirped parameter C, the second part $M_i(x, z, \omega)$ relies no not only observation point (x, z) and correlation length σ, but also oceanic parameters including mean square temperature dissipation rate χ_T, dissipation rate of turbulence kinetic energy in unit mass liquid ε, and relative intensity of temperature and salinity fluctuations ς.

The frequency ω_{max} of the maximum spectral intensities for the PCCAP and PCCGP beams are determined by

$$\frac{\partial S_i(x,z,\omega)}{\partial \omega}=0,\ (\text{i}=a\ or\ g). \tag{20}$$

The relative spectral shift is described by

$$\frac{\delta\omega}{\omega_0}=\frac{\omega_{max}-\omega_0}{\omega_0}. \tag{21}$$

If $\delta\omega>0$ the spectrum is blue-shifted, whereas it is red-shifted for $\delta\omega<0$.

Numerical calculations are performed to illustrate the influence of pulse duration T and chirped parameter C, observation point (x, z) and oceanic parameters (i.e. χ_T, ε, ς) on spectral behaviors of PCCAP and PCCGP beams. The calculation parameters are fixed to a=0.5, λ_0=532 nm, x_0=5 mm, σ=0.9 cm, z=500 m, C=2, T=3 fs, ς=−2.5, $\chi_T=10^{-9}$ K^2/s, $\varepsilon=10^{-6}$ m^2/s, $\eta=10^{-3}$ m, $\omega_0=2\pi c/\lambda_0$ and $c=3\times10^8$ m/s unless the other values are specified in the caption.

Fig.1 shows the relative spectral shifts of the PCCAP and PCCGP beams versus transverse coordinate x for different C and T. In the range of $0\le x\le30$ cm, one can see that their spectrums show slight blue shift at x=0, and the spectrum of PCCGP beam becomes red-shifted with an increase of off-axis distance of transverse coordinate x. Although the spectrum of PCCAP beam presents oscillating behavior near optical axis, its spectrum varies from blue-shifted to red-shifted to blue-shifted as the off-axis distance increases. In addition, there are some critical positions x_c where the value of red-shifted reaches the maximum. For example, for C=0, C=2 and C=4 of PCCAP beams in Fig.1(a) their maximal red shifts are −0.60, −0.59 and −0.54 at the critical positions x_c=7.5 cm, x_c=9.2 cm and 15.5 cm, respectively. The values of the critical positions x_c decrease with C increase. As can be seen in Fig.1, the offset value of spectral shifts become larger as the chirped parameter C increase or pulse duration T decrease, which indicates that spectral shifts can be enhanced by a larger C or smaller T.

Figs.2(a)—(c) and Figs.2(e) and (f) show more detailed descriptions of normalized spectral intensities $S(\omega)$ at some critical positions, where these spectrums are all red-shifted. For the PCCAP beams the spectrum distribution displays cusp shaping rather than a Gaussian form, and the overlapping parts of these cusp spectrums gradually increase for different chirped parameters or pulse durations with the increasing of off-axis distance. It can be seen that the red shift of T=2 fs shows maximal red shift of −0.58 at x=7.8 cm, and it decrease to −0.564 at x=12.4 cm, while for T=5 fs the red shift are −0.1 and −0.564, and its shift is maximal at x=12.4 cm. One can even see their normalized spectral intensities are almost the same at x=30 cm in Figs.2(c) and (f). The detailed spectral intensities in Fig.2 show consistency with spectral shifts in Fig.1.

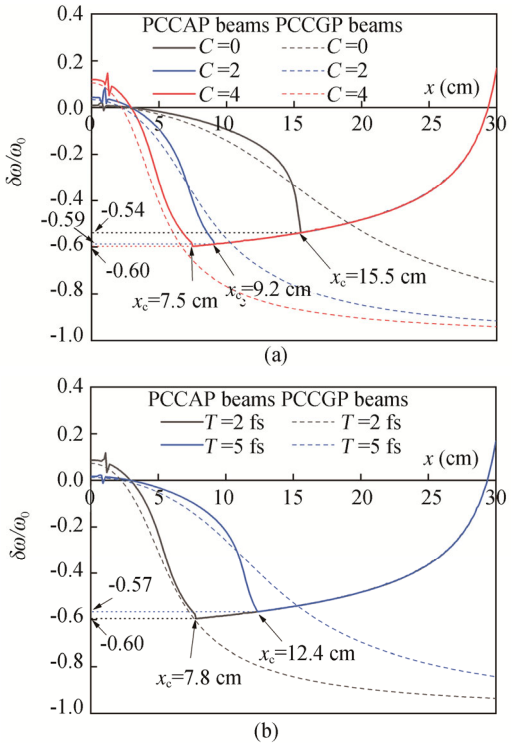

Fig.1 Relative spectral shifts of the PCCAP and PCCGP beams versus transverse coordinate *x* for different (a) *C* and (b) *T*

Relative spectral shifts of the PCCAP and PCCGP beams versus transverse coordinate x for different correlation lengths σ and oceanic turbulences (i.e. ε, ς and χ_T) are given in Figs.3 and 4, respectively. It is also found that the spectral shifts the PCCGP beam move in a monotony way along red-shifted direction. However, its spectral shift of PCCAP beam is richer than that of PCCGP beam. As can be see that the spectrum of PCCAP moves from blue shifted to red shifted for $x<x_c$, and it gets a maximal red-shifted value at $x=x_c$, and then it tends to move toward the direction of blue-shift for $x>x_c$ with a growing off-axis distance. A higher correlation length σ can acquire a larger red-shift. Furthermore, a higher ε or a smaller ς, χ_T has the ability to increase the offset value in red-shifts, but it shows less effect upon the change of spectral shifts $\Delta(\delta\omega/\omega_0)$ in range of $x>x_c$. For example, in the range of $x_c<x<25$ cm the changes of $\Delta(\delta\omega/\omega_0)$ are 0.05 and 0.9 for $\varepsilon=10^{-5}$ m^2/s and 10^{-7} m^2/s as shown in Fig.4(a), and their changes are 0.17 and 0.53 for ς=−4.5 and −1.5 in Fig.4(b), and the change value equals 0.07 and 0.6 for $\chi_T=10^{-10}$ K^2/s and 10^{-8} K^2/s in Fig.4(c).

It is worth noting that the rapid spectral transition of PCCAP beam in red-shifts appears at x=9.92 cm of

χ_T=10^{-8} K^2/s in Fig.4(c), where the transition is equal to 0.69. Fig.5 gives the physical explanation of the rapid spectral transition of PCCAP beam for the case of χ_T=10^{-8} K^2/s in Fig.4(c). One can see that there exists only one spectral maximum S_{max1} at x=9 cm, but two spectral maximums S_{max1} and S_{max2} located at $(\omega_{max1}-\omega_0)/\omega_0$=−0.14 and $(\omega_{max2}-\omega_0)/\omega_0$=−0.69 appear when the off-axis distance increases to x=9.92 cm as shown in Fig.5(b). When the off-axis distance further increase to x=10.2 cm, the first spectral maximum S_{max1} disappears, but the second S_{max2} still keeps its maximal value. The phenomenon can be attributed to the competition of two peak spectrums. If one of them is suppressed, then its peak spectrum will disappear, and if their peak spectrums are equal, then two spectral maximums can be found. The spectrum of PCCGP beam is also compared in Fig.5. It is obviously seen that its spectrum is smooth, which indicates that the competition is absent from the spectrum of PCCGP beams.

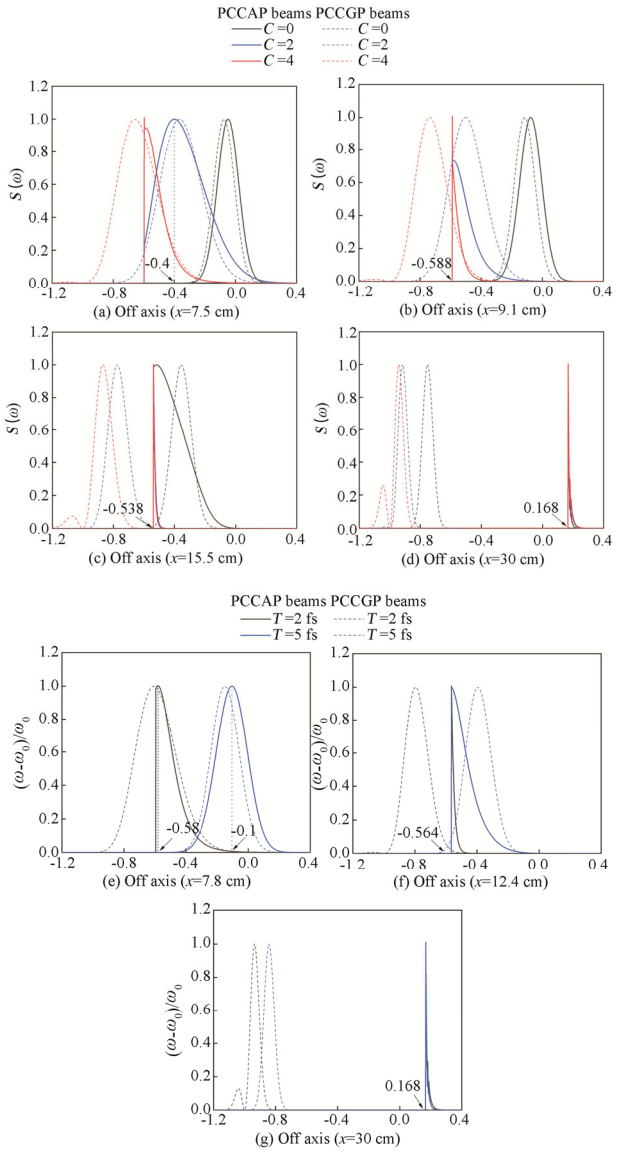

Fig.2 Normalized spectral intensities $S(\omega)$ at some critical positions for different C and T

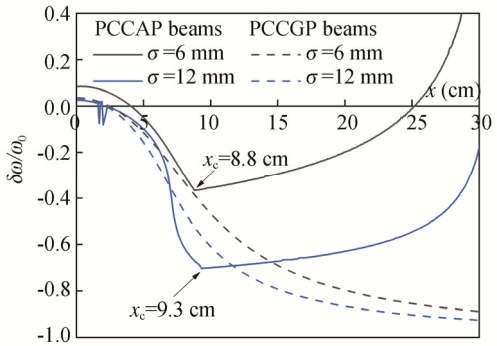

Fig.3 Relative spectral shifts of the PCCAP and PCCGP beams versus transverse coordinate x for different correlation lengths σ

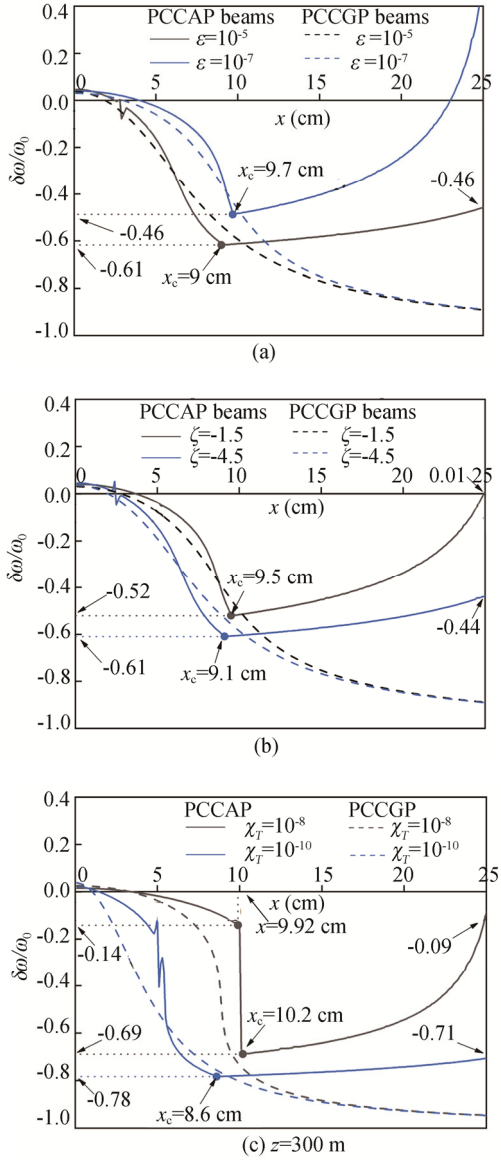

Fig.4 Relative spectral shifts of the PCCAP and PCCGP beams versus transverse coordinate x for different (a) ε, (b) ς and (c) χ_T

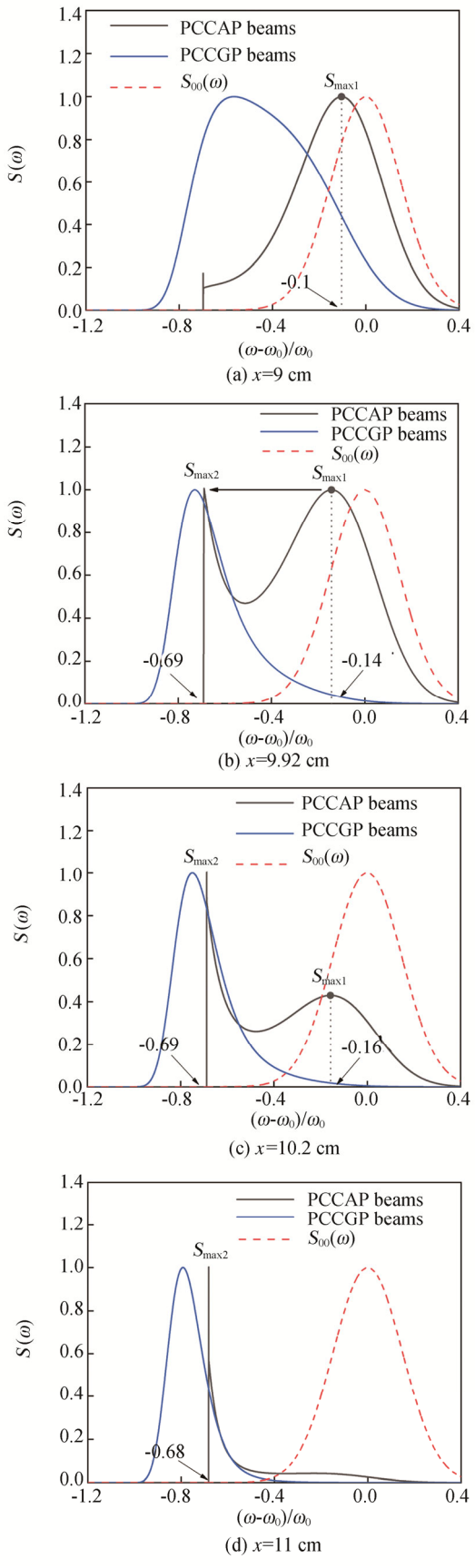

Fig.5 Physical explanations of the rapid spectral transition of PCCAP beam in Fig.4(c), where the spectrum of PCCGP beam is also compared

Based on the extended Huygens-Fresnel principle, the spectral properties of PCCAP beams propagating through oceanic turbulence are studied using approximate analytical spectral intensity expressions, where the spectrum of PCCGP beam is also compared. The influence of optical parameters including pulse duration T, chirped parameter C, correlation length σ and oceanic parameters (i.e. ε, ς and χ_T) on spectrum at observation point (x, z) is mainly discussed. The results show that the spectral shifts of PCCAP beam are richer than those of PCCGP beam. The spectrum of PCCAP beam is not a conventional Gaussian form, it gradually becomes sharp and eventually evolves into a cusp shape with increasing off-axis distance x. Furthermore, there exists some critical positions x_c for PCCAP beam where the spectral red-shifted reaches its maximum. For $x<x_c$ its spectrum moves from blue-shifted to red-shifted, while for $x>x_c$ the spectrum has a tendency to move toward the direction of blue-shifted with an increase of off-axis distance.

In addition, the spectral shifts in red-shifted increase with the increasing of chirped parameter C, correlation length σ or decreasing pulse duration T. Meanwhile, a larger value in red-shift can be also found by a higher ε or a smaller ς, χ_T. Finally, the appearance of a rapid spectral transition of PCCAP beam is also discussed and physically explained.

In comparison with Refs.[22, 23], where the intensity, coherence or statistical properties of partially coherent continuous beams were studied, while our attention is paid to partially coherent pulsed beams because their spectrums are wider than the cases of continuous beams. In such case spectral information encoding techniques can easily be employed. The results obtained here should be useful for underwater optical communication, imaging and sensing by selecting a suitable pulse duration, correlation length or chirped parameter in partially coherent pulsed beam.

References

[1] Johnson L J, Green R J and Leeson M S, Applied Optics **53**, 7273 (2014).

[2] Shchepakina E, Farwell N and Korotkova O, Applied Physics B **105**, 415 (2011).

[3] Tang Miao-miao and Zhao Dao-mu, Optics Communications **312**, 89 (2014).

[4] Huang Yong-ping, Zhang Bin, Gao Zeng-hui, Zhao Guang-pu and Duan Zhi-chun, Optics Express **22**, 17723 (2014).

[5] Lu L, Ji X L and Baykal Y, Optics Express **22**, 27112 (2014).

[6] Liu Da-jun, Wang Yao-chuan, Wang Gui-qiu, Yin Hong-ming and Wang Jin-ren, Optics & Laser Technology **82**, 76 (2016).

[7] Wu Yu-qian, Zhang Yi-xin, Li Ye and Hu Zheng-da, Optics Communications **371**, 59 (2016).

[8] Peng Xiao-feng, Liu Lin, Cai Yang-jian and Baykal YahYa, Journal of the Optical Society of America A **34**,

133 (2017).

[9] Ding Chao-lian, Feng Xiao-tong, Zhang Pei, Wang Hai-xia and Zhang Yong-tao, Journal of Physics: Conference Series **1053**, 012068 (2018).

[10] Liu Da-jun, Wang Yao-chuan, Wang Gui-qiu, Yin Hong-ming, Zhong Hai-yang and Wang Yao-chuan, Chinese Physics B **28**, 104207 (2019).

[11] Yang Yan-qiu, Yu Lin, Wang Qiu and Zhang Yi-xin, Applied Optics **56**, 7046 (2019).

[12] Wang Xin-guang, Zhen Yang and Zhao Sheng-mei, Optik **176**, 49 (2019).

[13] Liu Da-jun, Yin Hong-ming, Wang Gui-qiu and Wang Yao-chuan, Current Optics and Photonics **3**, 97 (2019).

[14] Zhang Qin-wei, Li Wen-dong, Liu Kai, Zhou Long-wen, Wang Zhao-ming and Gu Yong-jian, Journal of the Optical Society of America A **36**, 397 (2019).

[15] Sun Chao, Lv Xiang, Ma Bei-bei, Zhang Jian-bin, Deng Dong-mei and Hong Wei-yi, Optics Express **27**, A245 (2019).

[16] Liu Da-jun, Wang Gui-qiu, Yin Hong-ming, Zhong Hai-yang and Wang Yao-chuan, Optics Communications **43**, 346 (2019).

[17] Ye Feng, Xie Jin-tao, Hong Shi-han, Zhang Jian-bin and Deng Dong-mei, Results in Physics **13**, 102249 (2019).

[18] Jin Ying, Hu Ming-jun, Luo Mi, Luo Ynag, Mi Xian-wu, Zou Cheng-juan, Zhou Li-wang, Shu Cheng-fu, Zhu Xi-xiang, He Ju-xiang, Ouyang Sheng-de and Wen Wei, Journal of the Optical Society of America A **35**, 1457 (2018).

[19] Liu Da-jun and Wang Yao-chuan, Optics & Laser Technology **103**, 33 (2018).

[20] Luo Bin, Wu Guo-hua, Yin Long-fei, Gui Zhi-cheng and Tian Yue-han, Optics Communications **425**, 80 (2018).

[21] Huang Xian-wei, Deng Zhi-xiang, Shi Xiao-hui, Bai Yang-feng and Fu Xi-quan, Optics Express **26**, 4786 (2018).

[22] Liu Da-jun, Wang Gui-qiu, Yin Hong-ming, Zhong Hai-yang and Wang Yao-chuan, Optics Communications **437**, 346 (2019).

[23] Sun Chao, Lv Xiang, Ma Bei-bei, Zhang Jian-bin and Deng Dong-mei, Optics Express **27**, A245 (2019).

[24] Nelson W, Palastro J P, Davis C C and Sprangle P, Journal of the Optical Society of America A **31**, 603 (2014).

[25] Yan Xu, Guo Li-xin, Gong Teng and Cheng Ming-jian, Cross Strait Quad-Regional Radio Science and Wireless Technology Conference (CSQRWC), 2018.

[26] Jin Ying, Hu Ming-jun, Luo Mi, Luo Yang, Mi Xian-wu, Zou Chen-juan, Zhou Li-wang, Shu Cheng-fu, Zhu Xi-xiang, He Ju-xiang, OuYANG Sheng-de and Wen Wei, Journal of the Optical Society of America A **35**, 1457 (2018).

[27] Ji Xiao-ling, Zhang En-tao and Lü Bai-da, Journal of Modern Optics **54**, 541 (2007).

[28] Liu Da-jun, Wang Gui-qu and Wang Yao-chuan, Optics & Laser Technology **98**, 309 (2018).